Title

Radiologic progression of glioblastoma under therapy—an exploratory analysis of AVAglio

Journal

Neuro-Oncology, 20(4)

ISSN

1522-8517

Authors

Nowosielski, Martha

Ellingson, Benjamin M

Chinot, Olivier L

et al.

Publication Date

2018-03-27

DOI

10.1093/neuonc/nox162

Peer reviewed

Neuro-Oncology
20(4), 557–566, 2017 | doi:10.1093/neuonc/nox162 | Advance Access date 1 September 2017

Radiologic progression of glioblastoma under therapy—an exploratory analysis of AVAglio

Martha Nowosielski, Benjamin M. Ellingson, Olivier L. Chinot, Josep Garcia, Cedric Revil, Alexander Radbruch, Ryo Nishikawa, Warren P. Mason, Roger Henriksson, Frank Saran, Philipp Kickingereder, Michael Platten, Thomas Sandmann, Lauren E. Abrey, Timothy F. Cloughesy, Martin Bendszus, and Wolfgang Wick

Medical University Innsbruck, Department of Neurology, Innsbruck, Austria (M.N.); Aix-Marseille University, AP-HM, Service de Neuro-Oncologie, CHU Timone, Marseille, France (O.L.C.); University Medical Center, Neuroradiology, Heidelberg, Germany (A.R., P.K., L.E.A., M.B.); F. Hoffmann-La Roche Ltd, Basel, Switzerland (J.G., C.R.); Saitama Medical University, Saitama, Japan (R.N.); Princess Margaret Hospital, Toronto, Ontario, Canada (W.P.M.); Regional Cancer Center Stockholm and Umeå University, Stockholm and Umeå, Sweden (R.H.); The Royal Marsden NHS Foundation Trust, Surrey, UK (F.S.); UCLA Brain Tumor Imaging Laboratory and Neuro-Oncology Program, Los Angeles, California, USA (B.M.E., T.F.C.); University Medical Center, Neurology, and Neurooncology, German Cancer Research Center and the German Cancer Consortium, Heidelberg, Germany (M.N., M.P., W.W.); Neurology University Clinic, Mannheim, Germany (M.P.); Genentech, South San Francisco, California, USA (T.S.)

Corresponding Author: Martha Nowosielski, MD, PhD, or Wolfgang Wick, MD, Neurology Clinic and National Center for Tumor Diseases, University of Heidelberg and German Cancer Research Center, Im Neuenheimer Feld 400, D-69120 Heidelberg, Germany (Martha.Nowosielski@i-med.ac.at, wolfgang.wick@med.uni-heidelberg.de).

Abstract

Background. In this exploratory analysis of AVAglio, a randomized phase III clinical study that investigated the addition of bevacizumab (Bev) to radiotherapy/temozolomide in newly diagnosed glioblastoma, we aim to radiologically characterize glioblastoma on therapy until progression and investigate whether the type of radiologic progression differs between treatment arms and is related to survival and molecular data.

Methods. Five progression types (PTs) were categorized using an adapted algorithm according to MRI contrast enhancement behavior in T1- and T2-weighted images in 621 patients (Bev, $n = 299$; placebo, $n = 322$). Frequencies of PTs (designated as classic T1, cT1 relapse, T2 diffuse, T2 circumscribed, and primary nonresponder), time to progression (PFS), and overall survival (OS) were assessed within each treatment arm and compared with molecular subtypes and O^6-methylguanine DNA methyltransferase (*MGMT*) promoter methylation status.

Results. PT frequencies differed between the Bev and placebo arms, except for "T2 diffuse" (12.4% and 7.1%, respectively). PTs showed differences in PFS and OS; with "T2 diffuse" being associated with longest survival. Complete disappearance of contrast enhancement during treatment ("cT1 relapse") showed longer survival than only partial contrast enhancement decrease ("classic T1"). "T2 diffuse" was more commonly *MGMT* hypermethylated. Only weak correlations to molecular subtypes from primary tissue were detected.

Conclusions. Progression of glioblastoma under therapy can be characterized radiologically. These radiologic phenotypes are influenced by treatment and develop differently over time with differential outcomes. Complete resolution of contrast enhancement during treatment is a favorable factor for outcome.

Key words

bevacizumab | MRI | radiologic phenotypes | treatment resistance

Two recent phase III clinical studies in glioblastoma (GB), which although showing promising results for progression-free survival (PFS), failed to show a survival benefit with the addition of bevacizumab (Bev) to standard-of care therapy.[1,2] Understanding GB progression on therapy therefore constitutes a major aim in neuro-oncologic

Importance of the study

In neuro-oncological research, great attempts are being made to understand the biologic processes during glioblastoma progression. Unfortunately, longitudinal molecular analysis of glioblastoma tissue on or after therapy is rarely available. Using the imaging and clinical data from AVAglio, a randomized phase III clinical study that investigated the addition of bevacizumab to standard-of-care therapy in newly diagnosed glioblastoma, we radiologically characterized glioblastoma during progression. We here confirm data of a retrospective analysis which show that types of radiologic progression differ in time of appearance and are related to outcome. These progression types are unevenly distributed between the 2 treatment arms and may therefore be influenced by distinct therapies (anti-angiogenic vs sole cytotoxic/static treatment). By comparing these progression types to clinical and molecular data, understanding of these radiologic phenotypes is enhanced. Comprehension of glioblastoma progression under therapy might help in elucidating resistance mechanisms and guide subsequent therapy.

resistance research. Intriguing data on the clonal evolution of GB under therapy were recently presented,[3] emphasizing the need to characterize GB progression also radiologically.

In previous work, we defined MR based progression types (PTs) that differ with respect to time of appearance and clinical outcome in patients with recurrent GB following anti-angiogenic treatment with Bev.[4] PTs were defined on the pathophysiological basis that contrast enhancement (CE) reflects a disruption of the blood–brain barrier, and T2/fluid attenuated inversion recovery (FLAIR) signal changes display a mixture of leukoencephalopathy, infiltrating tumor, and edema. By analyzing CE development and T2 hyperintense signal changes during the course of treatment, different types of progression have been categorized.[4] We here describe 2 types of a solely T2-based tumor progression ("T2 diffuse" and "T2 circumscribed"), 2 T1 contrast enhancing phenotypes ("cT1 relapse" and "classic T1"), and a "primary nonresponder." We now aim to confirm the retrospective findings in the AVAglio trial, a phase III randomized, placebo-controlled, multicenter trial that was performed to study the therapeutic value of Bev in patients with newly diagnosed GB.[1] The cohort of this imaging substudy of AVAglio differs from the earlier retrospective cohort at recurrence in 2 aspects, namely the primary treatment setting and the presence of a non-Bev containing treatment arm, allowing us to investigate the following study aims. We aim (i) to investigate the frequency distribution of the PTs between the treatment arms and answer the question of whether PTs are specific to anti-angiogenic therapy or can also be seen during standard radiochemotherapy; (ii) to confirm previous associations of PTs with patient outcome; and (iii) to compare PTs with molecular expression subtype data and O^6-methylguanine DNA methyltransferase (*MGMT*) promoter methylation status.

Methods

Patients and Study Design

AVAglio was a randomized, double-blind, placebo-controlled phase III trial sponsored by F. Hoffmann-La Roche and conducted in accordance with the Declaration of Helsinki. The protocol was approved by local ethics committees and patients provided written informed consent. Full study design and outcomes have been published previously.[2] In brief, eligible patients were age >18 years with newly diagnosed supratentorial GB and World Health Organization performance score ≤2 and stable/decreasing corticosteroid dose during the 5 days prior to randomization. After debulking surgery, patients were randomly assigned at a ratio of 1:1 to receive radiotherapy (RT; 6 wk) in combination with daily temozolomide (TMZ) and Bev or placebo every 2 weeks. Following a 28-day treatment break, patients then received TMZ and Bev or placebo (for six 4-wk cycles), then single-agent Bev or placebo until progressive disease or unacceptable toxicity.

Patient Selection

Due to the specific definition of PTs, some patients had to be excluded from analysis (Supplementary Figure S1, consort diagram). For image analysis, 299 patients from the Bev + RT/TMZ and 322 from the placebo + RT/TMZ arms were included. Supplementary Table S1 provides an overview of patient characteristics of the imaging cohort.

Definition of Progression Types

PTs were assessed according to criteria previously published.[4] Of note, due to potential misleading of the formerly "cT1 flare-up" progression type and the "FLAIR" sequence in MRI, "cT1 flare-up" was renamed "cT1 relapse." MR images from start of therapy until tumor progression were reviewed for each patient and categorization of PTs was done according to CE behavior and T2/FLAIR signal changes during therapy. During image analysis, some imaging changes could not be attributed to one of the 4 PTs previously described,[4] and therefore a fifth PT had to be introduced. This is because this study population differs from the population of the original publication in 2 respects. First, in this analysis we are dealing with newly diagnosed GB patients, contrary to the retrospective analysis where we evaluated recurrent GB only and here >80% underwent complete or partial tumor resection. Secondly, the PTs from the original publication were defined on a population that was treated on an anti-angiogenic

basis only; here we have a placebo arm that is treated by cytotoxic therapy only, which might influence type of progression.

By this approach, 5 PTs were characterized: 2 according to T2/FLAIR signal changes ("T2 diffuse" and "T2 circumscribed"), 2 based mainly on CE changes on T1-weighted sequences ("cT1 relapse" and "classic T1"), and some patients showed tumor progression at first follow-up and were classified as "primary nonresponders."

In detail, "T2 diffuse" shows a complete decrease of CE during treatment. At progression these patients show a signal increase exclusively on T2/FLAIR-weighted images with a homogeneous signal pattern, signs of mass effect, excess of anatomical structures, and poorly defined borders on MRI. Hypointensity seen on T1-weighted images is faint and disproportionally smaller than T2 hyperintensity, or even not present at all. "T2 circumscribed" is characterized at tumor progression by either a complete decrease in CE on T1-weighted images or only a few faintly speckled CE lesions visible on cT1 images. In contrast to the T2 diffuse type, this T2/FLAIR hyperintense tumor progression is characterized by a bulky and inhomogeneous structure with sharp borders that correspond to a T1-hypointense signal seen on T1-weighted images.

"cT1 relapse" is characterized by a complete disappearance of CE on T1-weighted sequences (cT1) during treatment. At progression, however, a relapse of CE can be detected. "Classic T1" is the PT that was newly introduced. It differs from the cT1 relapse PT in that, although showing partial response or stable disease, there is no complete disappearance of CE during therapy. A CE decrease and stabilization during treatment can be detected with a subsequent increase at progression. As in cT1 relapse, T2 hyperintense signal decreases or stays stable and increases at progression. Primary nonresponders are defined by an increase and/or development of new CE lesions at first follow-up imaging after start of therapy. Image analysis was performed blinded to the treatment arms, survival dates, and the clinical course of the patients (Fig. 1, Supplementary Table S2).

Molecular Analysis

Data on *MGMT* promoter methylation status and molecular subtypes have been previously published,[1,5] and processed data on molecular subtypes were taken from the Gene Expression Omnibus database (hPFS://www.ncbi.nlm.nih.gov/geo/query/acc.cgi?acc5GSE84010).

Statistical Analysis

All results are reported as medians with 95% CIs for continuous variables and as frequencies or percentages for categorical variables. Univariate survival analyses used Kaplan–Meier methodology to generate median values. PFS, overall survival (OS), post-progression survival (PPS), and post-progression therapy were taken from the central review from the AVAglio trial and compared with PTs within one treatment arm. To compare molecular subtypes and PTs, a contingency table was generated and significant associations were calculated by chi-square test. In survival analysis, no multivariate analysis and no hazard ratios and *P*-values are shown, as this is an unplanned exploratory post hoc analysis with insufficient power for definitive conclusions (median and 95% CI are provided). *P*-values <0.05 are deemed statistically significant. Kaplan–Meier curves are based on the central review assessment of data, not on analyzer assessment. This is why some patients are censored in the PFS analysis (in these cases the analyzer defined tumor progression where the central reader did not yet see tumor progression). Due to central data acquisition closure and long survival of the T2 diffuse PT, median as well as upper 95% CI values may be missing and are marked by a star (*). Number of post-progression therapies may exceed patient number because post-progression therapy is not mutually exclusive, that is, some patients have received several therapies directly after progression. In order to avoid potential bias when selecting the "first" post-progression therapy, all data available on post-progression therapy are shown.

Results

Patient Characteristics

Basic characteristics are summarized in Supplementary Table S1. Clinical outcome data of the imaging cohort are in line with data on outcome of the original published study cohort. PFS and OS for the placebo arm are 6.13 months (5.87, 7.2) and 17.1 months (15.6, 18.9), respectively. PFS and OS for the Bev arm are 10.97 months (10.07, 12.0) and 17.33 months (15.57, 18.9), respectively.

Frequencies

In both treatment arms, the 5 PTs were detected, but at different frequencies, implying an influence of treatment on PT formation. Differences were detected between the 2 T1-based PTs and the T2 circumscribed PT. Interestingly, T2 diffuse, previously associated with being induced by Bev, was equally distributed between the treatment arms, suggesting a treatment-independent phenotype (Fig. 2, Supplementary Table S3).

Time to Development of Progression Type

Looking at the 2 treatment arms independently, median time from start of treatment until progression differed between the individual PTs in univariate analysis. Interestingly, in both treatment arms, differences between the 2 T1-based as well as the 2 T2-based progression patterns were detected, with T2 diffuse being the PT with longest PFS and cT1 relapse showing longer PFS than classic T1. The worst PFS in both arms (as per definition) was shown for the primary nonresponder. Importantly, there is no evidence that PFS, which differed between the treatment arms in the original study,[1] influenced the proportion of events per phenotype. In censored patients central review, investigator-assessed progression dates differ from our (blinded) analysis (Fig. 3, Table 1).

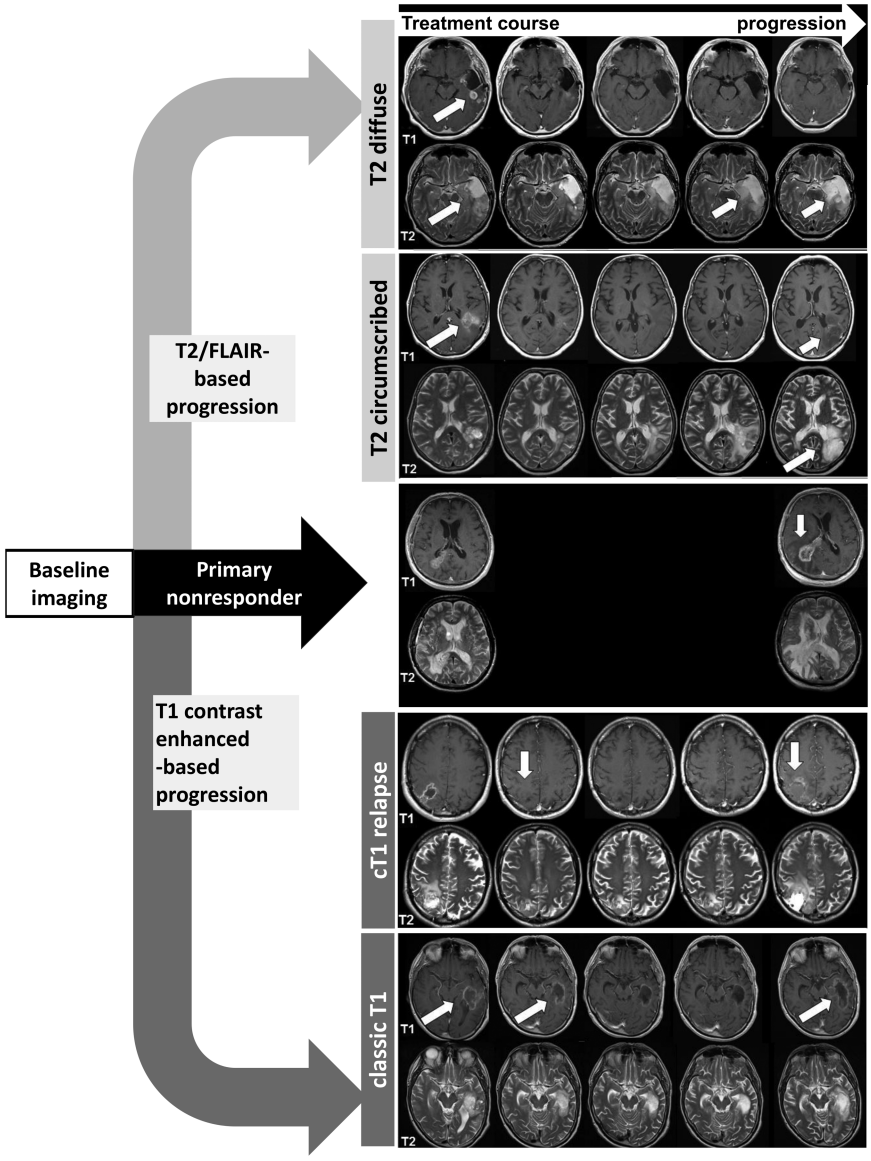

Fig. 1 Characterization of progression types. MR images from start of therapy until tumor progression were reviewed for each patient, and categorization of PTs was done according to CE behavior and T2/FLAIR signal changes during therapy. By this approach 5 PTs were characterized: 2 PTs mainly according to T2/FLAIR signal changes ("T2 diffuse" and "T2 circumscribed"), 2 PTs mainly based on CE changes on T1-weighted sequences ("cT1 relapse" and "classic T1"), and some patients showed tumor progression at first follow-up and were classified as "primary nonresponders." "T2 diffuse": CE is decreasing in T1-weighted images at first follow-up imaging after treatment initiation. T2 signal is also decreased; only faintly speckled contrast-enhancing lesions are visible at tumor progression. However, these patients show an increase exclusively in T2 hyperintensity, disproportionally larger than the T1 hypointensity, with a homogeneous signal pattern and poorly defined borders on MRI (white arrows). "T2 circumscribed": A decrease in CE on T1-weighted images is seen at first follow-up imaging after treatment initiation. At progression, a T2-hyperintense tumor progression with an inhomogeneous bulky structure and sharp borders corresponding to a T1-hypointense signal on T1-weighted images can be seen (white arrows). "cT1 relapse": A complete decrease in CE is visible on T1-weighted sequence during therapy. However, this CE increases again ("relapse") at tumor progression. T2 signal remains stable or increases. "Classic T1": An incomplete decrease of CE during therapy at T1-weighted sequences can be seen. At progression, this CE increases. T2 decreases or stays stable initially but increases at progression (white arrows). "Primary nonresponder": An increase in contrast enhancement is seen at first follow-up imaging after start of therapy. T2 signal stays stable or increases (white arrow).

Progression Type and Overall Survival

PTs within one treatment arm also show differences in median OS in univariate analysis. Interestingly, as for PFS, differences in OS were detected between the 2 T1-based progression patterns, and in the Bev arm even for the 2 T2-based PTs. Longest median OS was detected for the T2 diffuse PT, which did not reach median OS at data acquisition

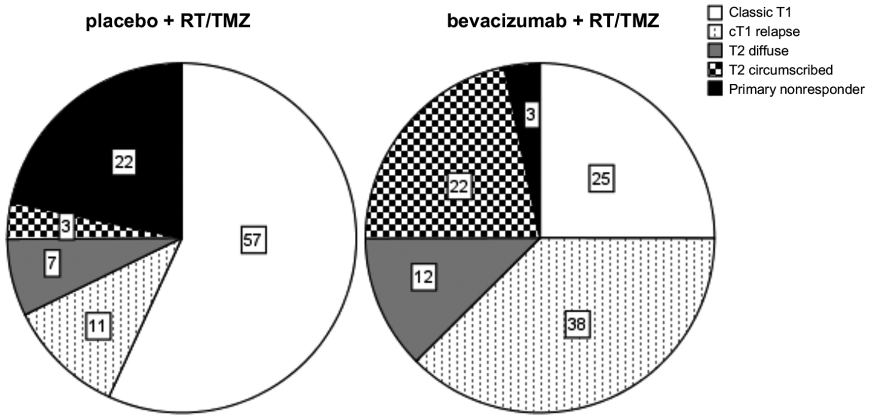

Fig. 2 Progression types and frequency distribution per treatment arm. In both treatment arms the 5 PTs were detected, but at different frequencies, implying an influence of treatment on PT formation. Significant differences were detected between the 2 T1-based PTs and the 2 T2 circumscribed PTs. Classic T1 progress and primary nonresponder were more common in the placebo than in the Bev arm (placebo 56.8% [51.4, 62.2] vs Bev 25.1% [20.2, 30.9], placebo 21.7% [17.2, 26.2] vs Bev 3.3% [1.3, 5.3], respectively). cT1 relapse as well as the T2 circumscribed PT were more commonly detected in the Bev than in the placebo arm (placebo 10.9% [7.5, 14.3] vs Bev 37.5% [32.9, 43.0], placebo 3.4% [1.4, 5.4] vs Bev 21.7% [17, 26.4], respectively). T2 diffuse was equally distributed between the treatment arms (placebo 7.1% [4.3, 9.9] vs Bev 12.4% [8.7, 16.1]), suggesting a treatment-independent phenotype.

closure; from Kaplan–Meier curves, however, a median OS >38 months (placebo arm) and >40 months (Bev arm) can be estimated. cT1 relapse showed longer median OS than classic T1 in both arms, and shortest median OS was detected for the primary nonresponders (Fig. 3, Table 1).

Progression Type and Post-Progression Survival and Therapy

In contrast to PFS and OS, no difference in PPS between the PTs was detected, as patients may have received several post-progression therapies (Table 1). Due to the study design, only a few post-progression scans are available to analyze whether PT characteristics were sustained and what effect post-progression therapy has on the individual PTs (Supplementary Table S4).

Progression Types and Molecular Analysis

MGMT

For our imaging cohort, methylation status was available in 469 (75.5%) patients: 250 (77.6%) patients in the placebo arm and 219 (73.2%) in the Bev arm (Supplementary Table S1). Interestingly, T2 diffuse was more commonly methylated than unmethylated in both treatment arms. All other PTs were more commonly unmethylated in both treatment arms, except for cT1 relapse, which was more commonly methylated in the placebo arm.

Molecular subtypes

Molecular subtype classification according to Sandmann et al[5] was available in 269 (43.3%) patients of our imaging cohort: 145 (54%) in the placebo arm, and 124 (46%) in the Bev arm. The only association between PT and molecular subtype was detected for the poorest subgroup—the primary nonresponders, who were associated with a proneural subtype in the placebo arm (15/30 proneural in the primary nonresponder PT, chi-square 27.6, $P = 0.036$; Table 2).

Discussion

In this post hoc analysis of AVAglio, 5 radiologic types of tumor progression, which vary in frequency depending on the treatment arm, are described. These PTs show differential outcomes, but only weak correlations were detected between PTs and molecular subgroups and *MGMT* status from primary tumor tissues.

Two patterns of a solely T2/FLAIR-based tumor progression, 2 patterns of a T1- contrast enhancing–based tumor progression, and a primary nonresponder were characterized. Progression types were defined on a simple basis of qualitatively assessing the decrease and increase of CE and T2/FLAIR hyperintense signal changes during therapy. These imaging features are the results of pathophysiological processes, such as blood–brain barrier breakdown for CE and tumor infiltration, oligodendrocyte/myelin damage, and edema for T2/FLAIR signal. Interestingly, frequencies of these PTs vary depending on the treatment arm. As expected, due to the impact of Bev on the blood–brain barrier, "cT1 relapse," characterized by a complete disappearance of CE during therapy and relapse at progression, was more commonly detected in the Bev arm. In contrast, "classic T1," characterized by an incomplete decrease of CE during treatment and CE increase at progression, was

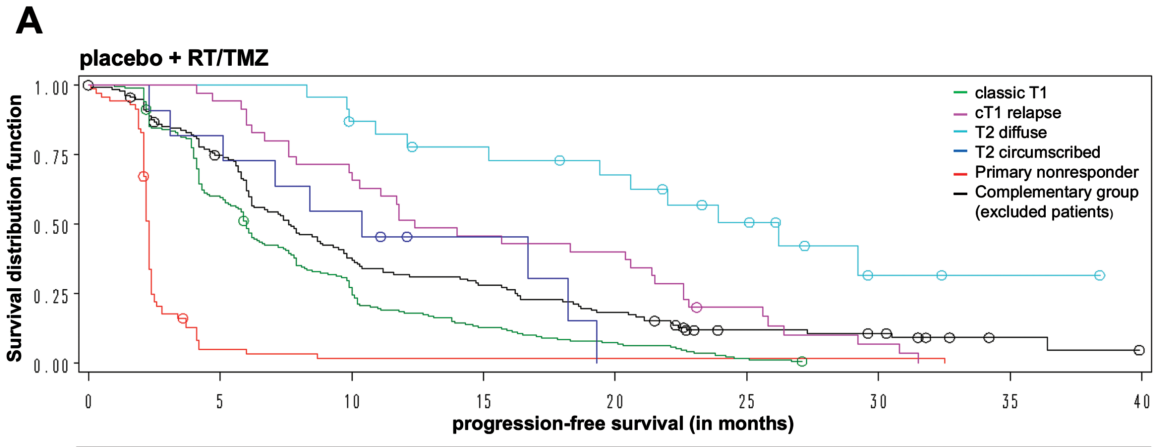

Patients at risk	STUDY MONTH															
	0	3	6	9	12	15	18	21	24	27	30	33	36	39	42	45
Classic T1	183	153	91	58	32	23	15	11	5	1	0	0	0	0	0	0
cT1 relapse	35	35	31	25	18	16	15	12	6	3	2	0	0	0	0	0
T2 diffuse	23	23	23	22	18	16	14	12	8	5	2	1	1	0	0	0
T2 circumscribed	11	10	8	6	4	3	2	0	0	0	0	0	0	0	0	0
Primary nonresponder	70	12	2	1	1	1	1	1	1	1	1	0	0	0	0	0
Complementary	141	114	86	56	42	37	29	22	10	10	8	3	2	1	0	0

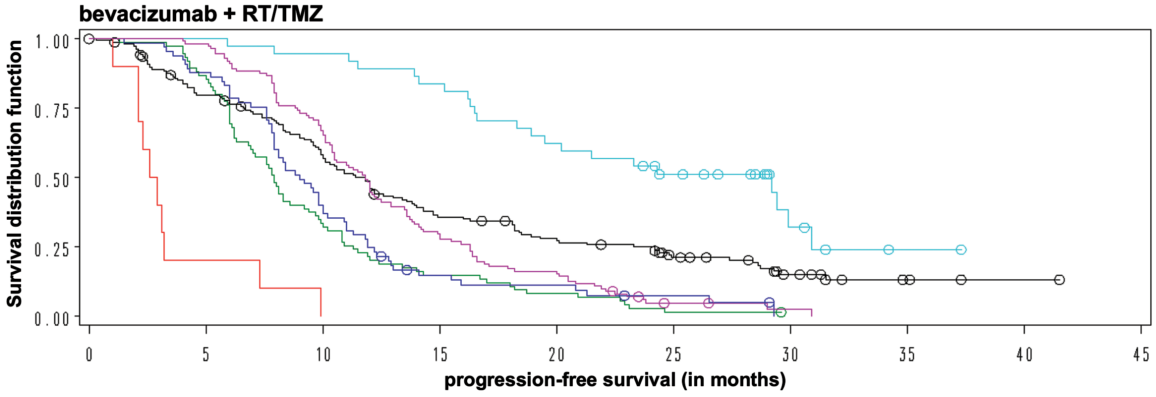

Patients at risk	STUDY MONTH															
	0	3	6	9	12	15	18	21	24	27	30	33	36	39	42	45
Classic T1	75	74	56	30	15	11	8	5	2	2	0	0	0	0	0	0
cT1 relapse	112	112	102	82	53	32	19	13	4	2	1	0	0	0	0	0
T2 Diffuse	37	37	36	35	33	31	26	22	19	13	5	2	1	0	0	0
T2 Circumscribed	65	64	53	32	16	8	6	5	3	2	0	0	0	0	0	0
Primary Nonresponder	10	4	2	1	0	0	0	0	0	0	0	0	0	0	0	0
Complementary	159	135	115	96	71	52	48	37	34	22	12	5	3	1	0	0

Fig. 3 Progression types and survival per treatment arm. (A) PFS. Median time from start of treatment until progression differed between the individual PTs in univariate analysis. Interestingly, in both treatment arms differences between the 2 T1-based as well as the 2 T2-based progression patterns were detected, with T2 diffuse being the PT with longest PFS and cT1 relapse showing longer PFS than classic T1. In the placebo arm, cT1 relapse showed significantly longer median PFS than the classic T1 PT (12.4 mo [10.0, 21.4] vs 6.0 mo [5.4, 7.2]), and T2 diffuse showed longer PFS than T2 circumscribed (26.2 mo [20.6, _._]* vs 10.4 mo [5.1, 18.2]). In the Bev arm, T2 diffuse showed significantly longer median PFS than all other PTs (29.3 mo [16.9, 30.9] vs classic T1 7.9 mo [6.9, 9.2] vs cT1 relapse 11.6 mo [10.4, 12.0] vs T2 circumscribed 9.1 mo [7.9, 10.0] and primary nonresponder 2.6 mo [2.1, 7.3]). Significant differences between the 2 T1-based progression patterns were also detected (median PFS 11.8 mo [10.4, 12.9] for cT1 relapse vs 7.9 mo [6.9, 9.2] for classic T1). The worst PFS in both arms (as per definition) was shown for the primary nonresponder (for more details, see Table 1). (B) OS. Progression types within one treatment arm also show differences in median OS in univariate analysis. In the placebo arm, significant differences in OS between the 2 T1 progression patterns could be detected, with cT1 relapse showing longer OS than the classic T1 (27.4 mo [21.6, 40.7] vs 16.8 mo [15.1, 19.1], respectively). T2 diffuse did not reach median OS at data acquisition closure; from Kaplan–Meier curve a median OS >38 months can be estimated. In the Bev arm, as estimated from the Kaplan–Meier curve, median OS in the T2 diffuse PT is >40 months, and therefore significantly longer than the OS from all other PTs (T2 circumscribed 13.6 mo [12.0, 15.2], cT1 relapse 17.8 mo [15.9, 20.5], classic T1 14.2 mo [12.9, 15.1]). In both arms, the shortest median OS was detected for the primary nonresponder (median OS 9.9 mo [7.9, 13.0] in the placebo arm, 9.6 mo [3.5, 12.3] in the bevacizumab arm).

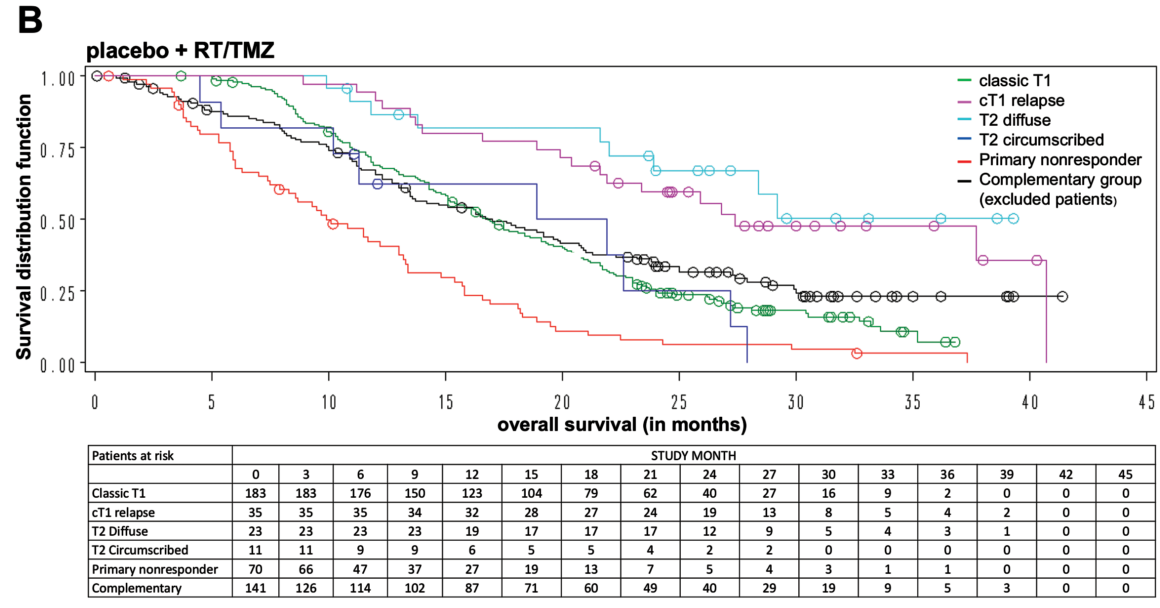

Patients at risk	STUDY MONTH															
	0	3	6	9	12	15	18	21	24	27	30	33	36	39	42	45
Classic T1	183	183	176	150	123	104	79	62	40	27	16	9	2	0	0	0
cT1 relapse	35	35	35	34	32	28	27	24	19	13	8	5	4	2	0	0
T2 Diffuse	23	23	23	23	19	17	17	17	12	9	5	4	3	1	0	0
T2 Circumscribed	11	11	9	9	6	5	5	4	2	2	0	0	0	0	0	0
Primary nonresponder	70	66	47	37	27	19	13	7	5	4	3	1	1	0	0	0
Complementary	141	126	114	102	87	71	60	49	40	29	19	9	5	3	0	0

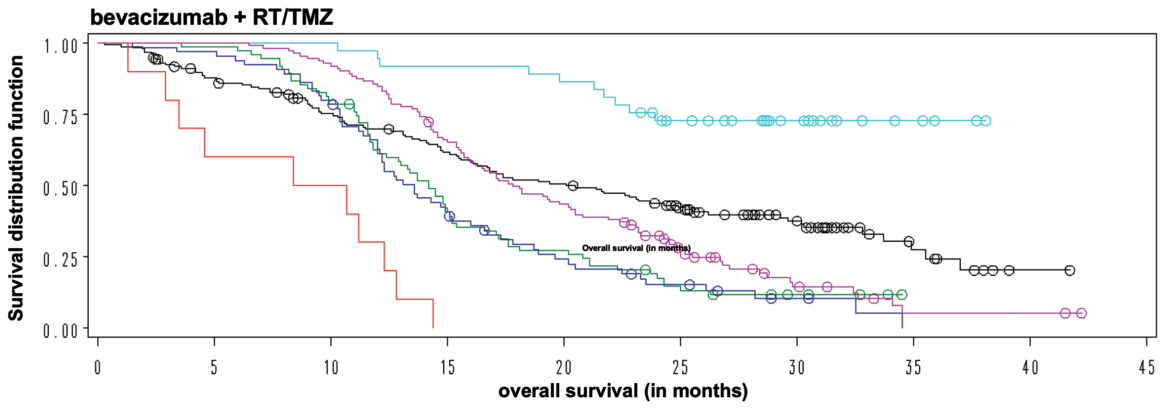

Patients at risk	STUDY MONTH															
	0	3	6	9	12	15	18	21	24	27	30	33	36	39	42	45
Classic T1	75	75	73	63	45	30	21	18	12	7	4	2	0	0	0	0
cT1 relapse	112	112	112	106	95	72	55	43	33	16	9	5	2	2	1	0
T2 Diffuse	37	37	37	37	35	34	32	25	19	12	5	2	0	0	0	0
T2 Circumscribed	65	64	61	56	41	26	17	12	8	5	3	1	0	0	0	0
Primary nonresponder	10	8	6	5	3	0	0	0	0	0	0	0	0	0	0	0
Complementary	159	144	131	117	103	90	76	71	61	44	33	14	6	2	0	0

Fig. 3 Continued

more commonly detected in the placebo arm, as was the "primary nonresponder." A radiologic phenotype characterized by a bulky T2 hyperintense signal with well-circumscribed borders and a matching T1 hypointensity, coined "T2 circumscribed," was more commonly seen in the Bev arm. Interestingly, "T2 diffuse," initially attributed to anti-angiogenic treatment, was equally distributed between the treatment arms, confirming prior analyses applying differential methods.[6,7] As PTs differ in frequency, depending on the treatment arm, it is now tempting to say that radiologic PTs have been induced or at least have been influenced by a specific therapeutic approach (anti-angiogenic based vs pure alkylating treatment). Recently, due to the advent of radiogenomics—the integration of imaging and genomic data—interesting associations between MR imaged macroscopic morphologic characteristics and biologic processes have been made.[8] By using a set of semi-quantitative radiographic descriptive features, differential protein expressions in incomplete versus complete contrast enhancing tumors were noted.[9,10] These studies show that contrast-enhancing tumors tend to have overexpression of genes associated with the hypoxia-angiogenesis-edema pathway (eg, vascular endothelial growth factor [VEGF], matrix metalloprotease 7).[9,10] As radiographic features such as development of CE are associated with biologic processes, we here hypothesize that the type of radiologic progression might represent tumor resistance mechanisms which have developed

Table 1 Progression type and survival per treatment arm

Treatment	Placebo RT/TMZ	Bevacizumab RT/TMZ	Placebo RT/TMZ	Bevacizumab RT/TMZ	Placebo RT/TMZ	Bevacizumab RT/TMZ
	PFS		OS		PPS	
	Median, mo (95% CI)		Median, mo (95% CI)		Median, mo (95% CI)	
Progression type						
ClassicT1	6.0 (5.3, 6.6)	7.9 (6.9, 9.2)	16.8 (15.1, 19.1)	14.2 (12.0, 15.1)	9.6 (7.8, 11.0)	5.7 (4.2; 6.9)
cT1 relapse	12.4 (10.0, 21.4)	11.8 (10.4, 12.9)	27.4(21.6, 40.7)	17.8 (15.9, 20.5)	13.9 (7.9, 14.9)	6.2 (5.0;7.5)
T2 diffuse	26.2 (19.4, _._*)	29.2 (18.9, 30.9)	_._ *(23.9, _._*)	_._*	5.6 (1.7, 18.6)	7.6 (4.4; _._*)
T2 circumscribed	10.4 (5.1, 18.2)	9.0 (7.9, 10.0)	18.9 (10.2, 27.2)	13.6 (12.1, 15.2)	5.9 (2.9, 9.1)	3.8 (2.7;5.0)
Primary nonresponder	2.3 (2.2, 2.3)	2.8 (2.1, 3.2)	9.9 (7.9, 13.0)	9.6 (3.5, 12.3)	6.8 (5.2, 10.9)	4.7 (0.6;8.0)

Note: Median time from start of treatment until PFS and OS differed between the individual PTs in univariate analysis. In contrast to PFS and OS, no difference in PPS was detected between the PTs. Due to the post hoc setting, no *P*-values are provided. *Median OS not reached due to data acquisition closure. PFS = progression-free survival, OS = overall survival, PPS = post-progression survival.

Table 2 Progression types and molecular subgroups according to The Cancer Genome Atlas analysis

Placebo + RT/TMZ						
	PN	**N**	**Class**	**Mes**	**Unclass**	**Total**
Progression type						
ClassicT1	20	2	20	36	5	**83**
cT1 relapse	6	1	4	3	0	**14**
T2 diffuse	5	2	1	7	0	**15**
T2 circumscribed	0	0	1	1	1	**3**
Primary nonresponder	**15**	4	5	4	2	**30**
	46	**9**	**31**	**51**	**8**	**145**
Chi-square = 27.6 degrees of freedom = 16 probability = 0.036						
Bevacizumab + RT/TMZ						
	PN	**N**	**Class**	**Mes**	**Unclass**	**Total**
Progression type						
ClassicT1	11	1	8	8	0	**28**
cT1 relapse	12	1	13	17	4	**47**
T2 diffuse	9	1	5	3	3	**21**
T2 circumscribed	7	0	3	11	3	**24**
Primary nonresponder	1	0	2	1	0	**4**
	40	**3**	**31**	**40**	**10**	**124**
Chi-square = 14.1 degrees of freedom = 16 probability = 0.589						

Note: Molecular subtype classification according to Sandmann et al[5] shows an association between primary nonresponders and the proneural subgroup but only in the placebo arm (15/30 proneural in the primary nonresponder PT . PN = proneural, N = neural, class = classical, mes = mesenchymal, unclass = not classified.

during therapy. Activation and/or upregulation of VEGF-independent pro-angiogenic signaling pathways have been shown to reestablish tumor neovascularization and provoke tumor relapse.[11–13] As these newly formed vessels have a disrupted blood–brain barrier and thus provoke CE on T1-weighted MRI scans, we hypothesize that this resistance mechanism might be depicted in the 2 T1-based PTs. Stereotactic biopsies performed in abnormal FLAIR areas on MRI revealed infiltrative tumor cells with areas of thin-walled blood vessels[14] which might be the pathophysiological background for the 2 T2-based PTs. De Lay et al support our hypothesis by showing that non-enhancing Bev-resistant GB and enhancing Bev-resistant GB have different molecular features.[15] Scribner et al presented a new pattern of tumor recurrence/resistance to Bev, associated with poor survival times, that radiologically manifested by an expanding area of necrosis and FLAIR signal in the absence of signal enhancement,[16] and serial stereotactic biopsies of high-grade astrocytomas revealed a differential spatial expression of VEGF.[17] Histopathologic correlations with tissue analysis from posttreatment tumor would strengthen our understanding of the radiologic PTs and enhance comprehension of GB progression in more detail, with the ultimate goal to guide post-progression therapy.

The second major finding of our study is that PTs develop differently over time and are associated with differential outcomes, confirming 2 retrospective analyses on radiologic PTs in recurrent GB.[4,18] The intrinsic challenge of our concept is to understand the implication of a radiologic phenotype, which is assessed at progression, and treatment outcome. Two clinically relevant points, however, may be discussed from this outcome analysis. First, we could show that independently of the treatment arm, "cT1 relapse" shows longer survival than "classic T1," indicating that a complete resolution of CE

during treatment has a better outcome than only a partial decrease of CE. Volumetric analysis of the AVAglio cohort supports our findings, where Ellingson et al demonstrated that CE decrease at first follow-up imaging is favorable for survival.[19] In this context it is reasonable to speculate that this observation (complete resolution of CE) might inform response assessment and refine commonly used tools such as the Response Assessment in Neuro-Oncology (RANO) criteria. Secondly, this study noted that up to 20% of patients (depending on the treatment arm) experience a solely T2/FLAIR hyperintense tumor progression, which strengthens the RANO criterion "significant T2/FLAIR signal increase" to define progression. We also confirm prior study results on different outcomes for the 2 T2/FLAIR-based PTs, with longest survival reported for the "T2 diffuse" PT in both treatment arms. From a biologic point of view T2 diffuse has to differ intrinsically from the other PTs, as it is not influenced by therapy and is more commonly MGMT methylated. As a limitation, this might be a confounder for the prognostic impact of the T2 diffuse PT, but might here be used as an interesting biologic observation. *MGMT* promoter methylation,[20] an epigenetic alteration, has also shown to be outcome related[21] and predictive for TMZ response. Whether *MGMT* methylation status only is responsible for the survival benefit of "T2 diffuse" is difficult to say, as we are limited in our statistical analysis to a univariate analysis and descriptive presentation of data due to the post hoc setting. However, no survival benefit for *MGMT* hypermethylated patients was reported for the AVAglio trial[1] and despite being more commonly unmethylated, cT1 relapse in the Bev arm showed survival times comparable to the T2 diffuse type.

Molecular subtypes, constituting a classification scheme, based on the resemblance to a distinct set of tissues that are enriched for markers of different aspects of tissue growth, have shown to be predictive of Bev treatment outcome.[5] For our imaging cohort, molecular subtype analysis was available in 246 patients (representing 46% of the whole imaging cohort), and we found a weak but statistically significant association between primary nonresponders and a proneural subtype in the placebo arm. This is an interesting finding, as patients with the proneural subtype had the worst prognosis in the Sandmann study and conversely were the one group with an OS benefit from Bev.[5] Recent molecular studies investigating longitudinal genomic and transcriptomic data from 114 recurrent GB patients show a highly branched evolutionary pattern in which more than half of patients experience an expression-based subtype change compared with the primary tumor[3] and it was shown that molecular subtypes may also change at progression.[22] This might explain the weak correlation between biology of primary tumor tissue and radiologic phenotype at progression, and imaging correlation studies with tissue from recurrent tumor are definitely needed and may give more conclusive results on underlying tumor biology.

In contrast to our previous findings we did not detect any association between PTs and PPS, which is most probably due to the fact that post-progression therapies influenced this time interval in this primary study cohort more than in the recurrent setting. As patients may have received multiple therapies after progression, we also failed to show a clear benefit for one PT to a specific therapy.

Limitations of this study are mainly due to the post-hoc statistical setting, allowing mostly a descriptive presentation of results. However, the goal of our study was not to provide prognostic parameters for differential treatment outcome; we here describe a radiologic pattern of tumor progression that might help us understand GB progression during therapy and guide post-progression therapy in the future. Chronologically, it is not possible to compare PTs and survival between the treatment arms (which is only possible within one arm). From the different frequencies of PTs by treatment arm, one can assume that the treatment may have an influence on the likelihood of patients to develop one or another type of tumor progression. Hence, if a patient is given placebo, this very same patient may not end up with the same PT if given Bev. Therefore, when comparing patients within one PT between Bev and placebo, we may not be looking at patients who are comparable before the PT classification operated by the drug given to the patient.

In summary, we confirm previous data that GB progression can radiologically be categorized into distinct phenotypes. These phenotypes seem to be influenced by treatment, as they show varying frequencies in the 2 treatment arms. Progression types develop differently over time with differential outcomes. Complete resolution of contrast enhancement during treatment is a favorable factor for outcome. "T2 diffuse," characterized by longest survival, seems to be a treatment-independent phenotype and shows associations with *MGMT* methylation status. Histopathologic correlation studies from recurrent GB tissue are further warranted to understand these progression types in more detail.

Supplementary Material

Supplementary material is available at *Neuro-Oncology* online.

Funding

The AVAglio trial was sponsored by F. Hoffmann-La Roche Ltd. The sponsor was involved in trial design, coordination of data collection, data analysis and interpretation, writing of the report, and provision of bevacizumab. The present post hoc analysis was performed from academic resources and was not part of the sponsored trial. All authors contributed to writing and approval of the manuscript. The corresponding author had final responsibility for the decision to submit for publication.

Acknowledgments

The authors confirm the originality of this study. Part of the results have been presented at the ASCO annual meeting 2016.

Conflict of interest statement:
B.E. is a paid consultant for Genentech/Roche, Siemens Medical, Agios, MedQIA, Nativis, Medicenna, Janssen Pharmaceuticals, Northwest Biotherapeutics, and Bristol-Myers Squibb and has received research grant funding from Genentech/Roche, Janssen Pharmaceuticals, and Siemens Medical.
O.L.C. is a paid consultant for Roche, Ipsen, Celldex, Immatics, and Bristol-Myers Squibb and has received research grant funding from Roche.
J.G. is a full time employee at F. Hoffmann-La Roche.
C.R. is a full time employee at F. Hoffmann-La Roche.
A.R. has served as a consultant for Guerbet, Bayer, GE, Bracco, and AbbVie; received financial study support by Guerbet and Bayer and received speaker honoraria from Guerbet, Bayer, Siemens, and Prime Oncology.
R.N. has received personal fees from Eisai, MSD, F. Hoffmann-La Roche and Chugai.
W.P.M. is a paid consultant for Roche and MSD and has received grant funding from Roche.
F.S. has received personal fees and nonfinancial support from F. Hoffmann-LaRoche.
M.P. has participated in a speaker's bureau for Novartis, Merck, and Teva. He has received research funding from Pfizer and has a consultant relationship with Genentech/Roche and Novartis.
M.B. has received speaker honoraria and research funding from Novartis, Bayer, Codman, Teva, Roche, Siemens, Guerbet, Stryker, and Medtronic and has a consultant relationship with Boehringer Ingelheim, B. Braun, and Guerbet.
T.S. is a full time employee at F. Hoffmann-La Roche.
L.E.A. is a full time employee at F. Hoffmann-La Roche.
T.F.C. has a consultant relationship with Tocagen, Pfizer, Roche/Genentech, Notable Labs, ProNAI, Life Sciences, VBL, Wellcome Trust, Agios, BMS, Merck, Cancer Panels, Insys, Human Longevity, Sunovion, Boston Biomedical, Alexion, Novogen, and Novocure and has stock options for Notable Labs.
W.W. has participated in a speaker's bureau for and has received research funding from MSD. He has received research funding from Apogenix, Boehringer Ingelheim, Genentech Roche, and Pfizer and has a consultant relationship with BMS, Celldex, MSD, and Genentech/Roche.
Authors not in this statement report no conflict of interest.

References

1. Chinot OL, Wick W, Mason W, et al. Bevacizumab plus radiotherapy-temozolomide for newly diagnosed glioblastoma. *N Engl J Med*. 2014;370(8):709–722.
2. Gilbert MR, Dignam JJ, Armstrong TS, et al. A randomized trial of bevacizumab for newly diagnosed glioblastoma. *N Engl J Med*. 2014;370(8):699–708.
3. Wang J, Cazzato E, Ladewig E, et al. Clonal evolution of glioblastoma under therapy. *Nat Genet*. 2016;48(7):768–776.
4. Nowosielski M, Wiestler B, Goebel G, et al. Progression types after antiangiogenic therapy are related to outcome in recurrent glioblastoma. *Neurology*. 2014;82(19):1684–1692.
5. Sandmann T, Bourgon R, Garcia J, et al. Patients with proneural glioblastoma may derive overall survival benefit from the addition of bevacizumab to first-line radiotherapy and temozolomide: retrospective analysis of the AVAglio trial. *J Clin Oncol*. 2015;33(25):2735–2744.
6. Wick A, Dörner N, Schäfer N, et al. Bevacizumab does not increase the risk of remote relapse in malignant glioma. *Ann Neurol*. 2011;69(3):586–592.
7. Wick W, Chinot OL, Bendszus M, et al. Evaluation of pseudoprogression rates and tumor progression patterns in a phase III trial of bevacizumab plus radiotherapy/temozolomide for newly diagnosed glioblastoma. *Neuro Oncol*. 2016;18(10):1434–1441.
8. Ellingson BM. Radiogenomics and imaging phenotypes in glioblastoma: novel observations and correlation with molecular characteristics. *Curr Neurol Neurosci Rep*. 2015;15(1):506.
9. Pope WB, Chen JH, Dong J, et al. Relationship between gene expression and enhancement in glioblastoma multiforme: exploratory DNA microarray analysis. *Radiology*. 2008;249(1):268–277.
10. Diehn M, Nardini C, Wang DS, et al. Identification of noninvasive imaging surrogates for brain tumor gene-expression modules. *Proc Natl Acad Sci U S A*. 2008;105(13):5213–5218.
11. Bergers G, Hanahan D. Modes of resistance to anti-angiogenic therapy. *Nat Rev Cancer*. 2008;8(8):592–603.
12. Soda Y, Marumoto T, Friedmann-Morvinski D, et al. Transdifferentiation of glioblastoma cells into vascular endothelial cells. *Proc Natl Acad Sci U S A*. 2011;108(11):4274–4280.
13. Carmeliet P, Jain RK. Molecular mechanisms and clinical applications of angiogenesis. *Nature*. 2011;473(7347):298–307.
14. de Groot JF, Fuller G, Kumar AJ, et al. Tumor invasion after treatment of glioblastoma with bevacizumab: radiographic and pathologic correlation in humans and mice. *Neuro Oncol*. 2010;12(3):233–242.
15. DeLay M, Jahangiri A, Carbonell WS, et al. Microarray analysis verifies two distinct phenotypes of glioblastomas resistant to antiangiogenic therapy. *Clin Cancer Res*. 2012;18(10):2930–2942.
16. Scribner E, Saut O, Province P, Bag A, Colin T, Fathallah-Shaykh HM. Effects of anti-angiogenesis on glioblastoma growth and migration: model to clinical predictions. *PLoS One*. 2014;9(12):e115018.
17. Johansson M, Brännström T, Bergenheim AT, Henriksson R. Spatial expression of VEGF-A in human glioma. *J Neurooncol*. 2002;59(1):1–6.
18. Kim BS, Kim SK, Choi SH, et al. Prognostic implication of progression pattern after anti-VEGF bevacizumab treatment for recurrent malignant gliomas. *J Neurooncol*. 2015;124(1):101–110.
19. Ellingson BM, Garcia J, Revil C, et al. Residual tumor volume and change in tumor volume during adjuvant therapy to predict long-term survival in AVAglio: phase 3 newly diagnosed glioblastoma patients treated with radiation, temozolomide, and bevacizumab or placebo. *J Clin Oncol*. 2016;34(suppl; abstr 2021):2021–2021.
20. Hegi ME, Diserens AC, Gorlia T, et al. MGMT gene silencing and benefit from temozolomide in glioblastoma. *N Engl J Med*. 2005;352(10):997–1003.
21. Weller M, Tabatabai G, Kästner B, et al.; DIRECTOR Study Group. MGMT promoter methylation is a strong prognostic biomarker for benefit from dose-intensified temozolomide rechallenge in progressive glioblastoma: the DIRECTOR trial. *Clin Cancer Res*. 2015;21(9):2057–2064.
22. Phillips HS, Kharbanda S, Chen R, et al. Molecular subclasses of high-grade glioma predict prognosis, delineate a pattern of disease progression, and resemble stages in neurogenesis. *Cancer Cell*. 2006;9(3):157–173.